DOI: 10.1002/cmdc.200900309

Azetidinones as Zinc-Binding Groups to Design Selective HDAC8 Inhibitors

Paola Galletti,[a] Arianna Quintavalla,[a] Caterina Ventrici,[a] Giuseppe Giannini,*[b] Walter Cabri,[b] Sergio Penco,[b] Grazia Gallo,[b] Silvia Vincenti,[b] and Daria Giacomini*[a]

2-Azetidinones, commonly known as β-lactams, are well-known heterocyclic compounds. Herein we described the synthesis and biological evaluation of a series of novel β-lactams. In vitro inhibition assays against HDAC isoforms showed an interesting isoform-selectivity of these compounds towards HDAC6 and HDAC8. The isoform selectivity changed in response to modification of the azetidinone-ring nitrogen atom substituent. The presence of an *N*-thiomethyl group is a prerequisite for the activity of these compounds in the micromolar range towards HDAC8.

Introduction

Histone deacetylases are involved in determining the pattern of acetylation of chromatin proteins, histones, in eukaryotic cells. Since the discovery of the role of reversible acetylation of histone proteins in the regulation of gene expression,[1] 18 potential human histone deacetylases (HDACs) have been discovered. These can be divided into four classes (I–IV). Class I (HDAC1, -2, -3 and -8), class II (HDAC4, -5, -6, -7, 9, -10) and class IV (HDAC11) operate by zinc-dependent mechanisms; in contrast, class III HDACs use NAD^+ as a cofactor. Classes I and IV HDACs are ubiquitously expressed, are predominantly in the nucleus, and function mainly as transcriptional co-repressors that are linked to cell proliferation and survival.[2] The distribution of class II HDACs, which are able to shuttle in and out of the nucleus, is more tissue specific, suggesting distinct functions in cellular differentiation and developmental processes.[3]

Currently, a number of potential drugs are in clinical trials as HDAC inhibitors; the first FDA-approved compound was suberoylanilide hydroxamic acid (SAHA), a pan-HDACs inhibitor.[4] In terms of chemical structures, HDAC inhibitors include a wide range of scaffolds and can be classified in structural classes such as aliphatic acids, hydroxamic acids, cyclic peptides and benzamides. A well-accepted pharmacophore model for these inhibitors consists of: a) a capping group that interacts with the residues at the active site entrance; b) a zinc-binding group (ZBG) that coordinates to the catalytic metal atom within the active site; and c) a linker group that binds in a hydrophobic channel and positions the ZBG and a capping group for interactions in the active site (Figure 1).

Although the connections between certain HDAC isoforms and pathophysiology are still evolving, accumulating data suggest that targeting specific HDACs might be beneficial in treating certain disease conditions, while limiting side effects.[5a–d] Hence, the emerging trends are to develop novel HDAC class-specific inhibitors. Modification of the capping group, linker and ZBG individually contribute to selectivity towards specific HDAC isoforms. In spite of significant results obtained through modification of the cap group in the development of class-selective rather than isoform-selective inhibitors, similar results through modification of the ZBG have proved more difficult to obtain.

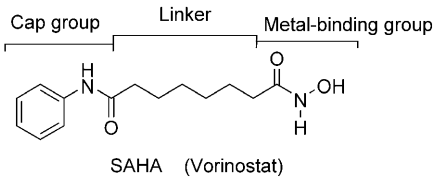

Figure 1. Modular structure of the HDAC inhibitor, SAHA.

Human HDAC8 is a class I hystone deacetylase that was first cloned by members of the Pharmacyclics HDAC team in 1999 and has been identified in a variety of human cancer tissues. Earlier studies suggested that HDAC8 localized to the nucleus and was ubiquitously expressed.[6a–c] Recently, it was demonstrated that HDAC8 is a novel, predominantly cytosolic marker of smooth muscle differentiation, including smooth muscle, myofibroblastic, and myoepithelial cells,[7] and may play an important role in neuroblastoma pathogenesis.[8] Additionally, HDAC8 is associated with the actin cytoskeleton in smooth muscle cells and regulates the contractile capacity.[9] This protein has also been linked to cancer as it is recruited by the leukemic inv[16] protein;[10] it regulates telomerase activity,[11] and siRNAs targeting HDAC8 were shown to have antitumor effects in cell culture.[12] Inhibition of the secretion of proinflammatory

[a] *Dr. P. Galletti, Dr. A. Quintavalla, Dr. C. Ventrici, Prof. D. Giacomini*
Dipartimento di Chimica "G. Ciamician"
Università of Bologna, Via Selmi 2, 40126 Bologna (Italy)
Fax: (+39) 051 2099456
E-mail: daria.giacomini@unibo.it

[b] *Dr. G. Giannini, Dr. W. Cabri, Dr. S. Penco, Dr. G. Gallo, Dr. S. Vincenti*
R&D Sigma-Tau S.p.A., Via Pontina, km 30400, 00040 Pomezia (Italy)
Fax: (+39) 06 91393638
E-mail: giuseppe.giannini@sigma-tau.it

Supporting information for this article is available on the WWW under http://dx.doi.org/10.1002/cmdc.200900309.

cytokines such as interleukin(IL)-1beta and IL-18 from peripheral blood mononuclear cells (PBMC) has been highlighted using selective HDAC8 inhibitors like PCI-34051.[13] HDAC8 is normally inhibited by the so-called pan-inhibitors, such as valproic acid (VPA), sodium butyrate (NaBu), trapoxin, SAHA, trichostatin A (TSA), PXD-101, LBH-589, LAQ-824.[14] Furthermore, some HDAC8-selective inhibitors were discovered by serendipity or designed ad hoc using co-crystal structures of inhibitors bound to HDAC8. The first crystal structure of a mammalian HDAC was published in 2004.[12–15] Analysis of the HDAC8 crystal structure in complex with an inhibitor containing an aryl linker (CRA-A) revealed a large subpocket in the side of the hydrophobic active site channel that was not apparent in the crystal structure of HDAC8 in complex with SAHA.[15] The HDAC inhibitor PCI-34051 was rationally designed with an indole present in the linker domain to specifically target this subpocket,[13] while SB-379278A was identified by an enzyme-based high-throughput screen (Figure 2).[16]

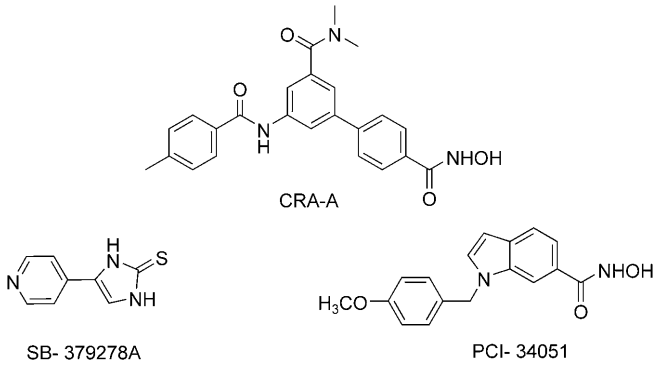

Figure 2. Known HDAC8-selective inhibitors.

β-Lactams are a very important class of bioactive molecules. Starting from the antimicrobial potency exerted by naturally occurring bicyclic compounds (penicillins and cephalosporins), nowadays new variants with monocyclic structures (azetidinones) are displaying new and specific biological activities.[17] β-Lactam-related compounds are irreversible inhibitors of a wide range of serine proteases, including elastases, β-lactamases, phospholipase A2, and bacterial signal peptidases.[18] Giacomini et al. have actively contributed to the development of this field with the synthesis of monocyclic β-lactams as scaffolds for antibiotics against resistant bacteria,[19] as enzymatic inhibitors against human leukocyte elastase (HLE) and matrix metallo-proteases (MMPs),[20] as antioxidants,[21] and as antiaggregating agents.[22] Some aryl-β-lactam derivatives have previously been evaluated for cytotoxicity against a number of human tumor and normal cell lines.[23] In particular N-thiolated β-lactams were found to induce DNA damage, cell growth arrest, and apoptosis in cultured human cancer cells.[24] Interestingly some bicyclic β-lactams were previously reported as HDAC inhibitors.[25]

In a research project aimed at the identification of new selective HDAC inhibitors, we found that some azetidinone derivatives showed good affinity and specificity towards HDAC8.

The design of β-lactams described herein was based on the modular structure as described for SAHA (Figure 1). An azetidin-2-one ring was identified as metal-binding group, a saturated or unsaturated chain as the linker, and the capping group was typical of those seen in compounds such as SAHA or *p*-phenylcinnamyl esters.[26a,b] The cap–linker module is anchored on the β-lactam ring at one of the two side chains; the substituent on the β-lactam nitrogen atom is the second source of molecular diversity and we synthesized *N*-H, *N*-OH, *N*-SMe and *N*-*o*-aminophenyl derivatives for a specific evaluation of the β-lactam core as a metal-binding group (compounds **1**–**9**). Our findings validate *N*-thiomethyl-β-lactam as a new Zn-binding group in the design of new selective HDAC8 inhibitors.

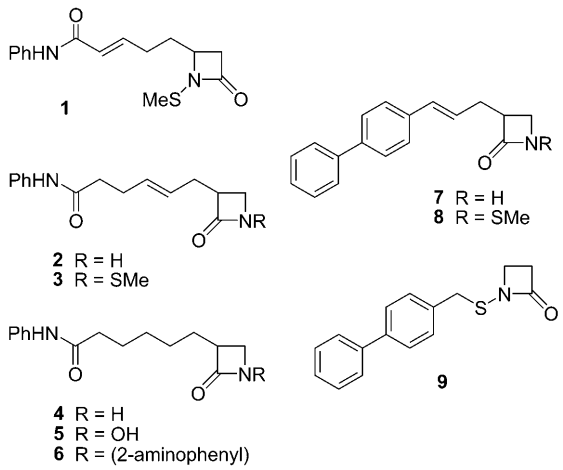

Results and Discussion

Chemical synthesis

The synthesis of β-lactams required careful design of the synthetic strategies because of the sensitivity of the four member ring to harsh reaction conditions, and regio- and chemoselectivity problems due to the presence of peculiar functional groups.

The synthesis of azetidinone **1** was achieved as shown in Scheme 1. Starting from the commercially available 4-acetoxy-azetidin-2-one, we obtained 4-benzenesulfonyl-azetidin-2-one

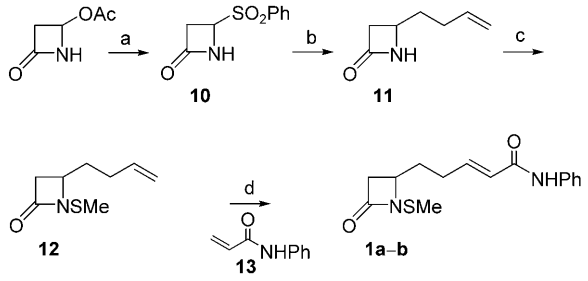

Scheme 1. *Reagents and conditions*: a) $PhSO_2Na$, DMF, 0 °C→RT; b) but-3-enyl-MgBr, THF, −78 °C→RT; c) 1. LiHMDSA, THF, −78 °C; 2. $MeSO_2SMe$; d) Grubbs II (5 mol%) CH_2Cl_2, reflux.

10 in 77% yield. Nucleophilic substitution with but-3-enylmagnesium bromide afforded the 4-butenyl-azetidinone **11**. N-Thiomethylation by deprotonation with lithium hexamethyl disilylamide (LiHMDSA) and subsequent reaction with $MeSO_2SMe$ gave **12** in 94% yield. Cross-metathesis with *N*-phenylacrylamide **13** in the presence of Grubbs 2nd-generation catalyst (benzylidene[1,3-bis(2,4,6-trimethylphenyl)-2-imidazolidinylidene]dichloro(tricyclohexylphosphine)ruthenium) afforded the racemic *N*-thiomethyl-azetidinone **1** in 51% yield. The two enantiomers were separated by semi-preparative chiral HPLC (see Experimental Section for details).

The synthesis of azetidinones **2**, **3**, and **4** is shown in Scheme 2. Starting from commercially available β-alanine in the presence of an excess of LiHMDSA and allyl bromide, we obtained the 2-allyl-β-alanine **14** in 53% yield. Base-catalyzed cyclization afforded the 3-allyl-azetidin-2-one **15** in 66% yield. Cross-metathesis with pent-4-enoic acid phenylamide **17** gave **2** in 58% yield. Compound **2** was predominantly obtained as the *E* isomer with only traces of the *Z* isomer evidenced by chiral HPLC. Again, separation of the four stereoisomers was achieved using chiral HPLC (see Experimental Section). Palladium-catalyzed hydrogenation gave the azetidinone **4** in quantitative yields. Insertion of the *N*-thiomethyl group in **4** is difficult because a competition occurs between the lactam and the amide group in the side chain. However, N-thiomethylation of **15** successfully gave **16**, which was subsequently reacted with amide **17** to give azetidinone **3** in a 37% yield (two steps). Compound **3** was predominantly obtained as the *E* isomer with only trace amounts of the *Z* isomer, but semi-preparative chiral HPLC allowed the separation of the four stereoisomers (see Experimental Section).

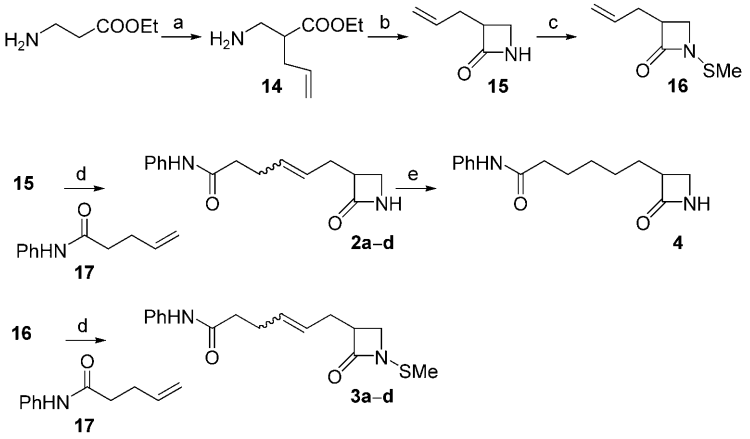

Scheme 2. *Reagents and conditions*: a) 1. LiHMDSA, THF, −78 °C; 2. allyl bromide, THF; b) LiHMDSA, THF, −78 °C→0 °C; c) 1. LiHMDSA, THF, −78 °C; 2. $MeSO_2SMe$; d) Grubbs II (5 mol%), CH_2Cl_2 reflux; e) H_2, Pd-C, THF/MeOH.

Cross-metathesis of 3-allyl-azetidinones **15** and **16** was successful, even with 4-vinylbiphenyl, giving compounds **7** and **8**, respectively (Scheme 3).

The *N*-hydroxy-azetidinones **5a–b** contain a hydroxamic acid scaffold in a cyclic form. Scheme 4 illustrates the preparation

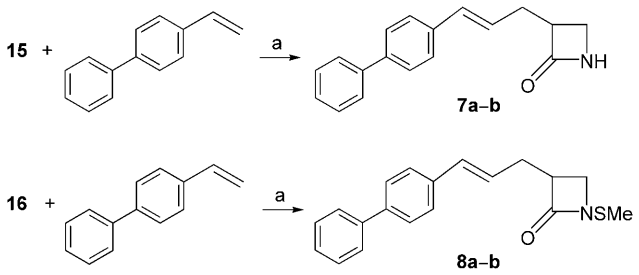

Scheme 3. *Reagents and conditions*: a) Grubbs II (5 mol%), CH_2Cl_2, reflux.

of *N*-hydroxy-azetidinone **5**. Starting from methyl-4-pentenoate, enolization and subsequent hydroxymethylenation with formaldehyde gave **18** in 42% yield. Acyl substitution by *O*-benzyl-hydroxylamine afforded derivative **19** (yield = 48%). Cyclization with diisopropylazodicarboxylate (DIAD) and triphenylphosphine resulted in azetidinone **20** in excellent yield (96%). Cross-metathesis with pent-4-enoic acid phenylamide **17** and subsequent hydrogenolysis with Pd-C gave the *N*-hydroxyazetidinone **5**, which was separated into the two enantiomers by semi-preparative chiral HPLC.

The *N*-*o*-aminophenyl-azetidin-2-one **6** was prepared with a four-step synthesis starting from the hydroxyester **18** (Scheme 5). Cross metathesis of **18** with amide **17** resulted in compound **22** (yield = 47%). Acyl substitution with *ortho*-carbobenzyloxy-amino-aniline (**23**) gave **24** in 67% yields. Cyclization with DIAD gave the azetidinone **25** in 77% yields. Hydrogenolysis (Pd-C) quantitatively resulted in the *N*-*o*-aminophenyl-azetidin-2-one **6**. 1-(Biphenyl-4-yl-methylsulfanyl)azetidin-2-one **9** was obtained in 84% yield starting from the commercially available azetidin-2-one, deprotonation with LiHMDSA and reaction with **26** (Scheme 6).

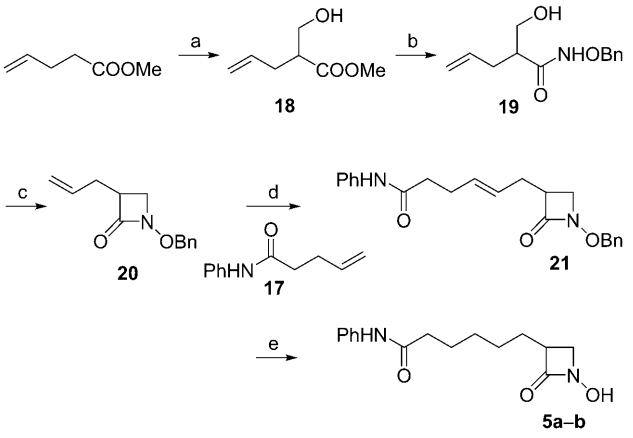

Scheme 4. *Reagents and conditions*: a) 1. LDA, THF, −78 °C; 2. $HCHO_{(g)}$, −60 °C→RT; b) $BnONH_2$·HCl, LiHMDSA, THF, −78 °C→RT; c) DIAD, Ph_3P, THF, RT; d) Grubbs II (5 mol%), CH_2Cl_2, reflux; e) H_2, Pd-C, THF/MeOH.

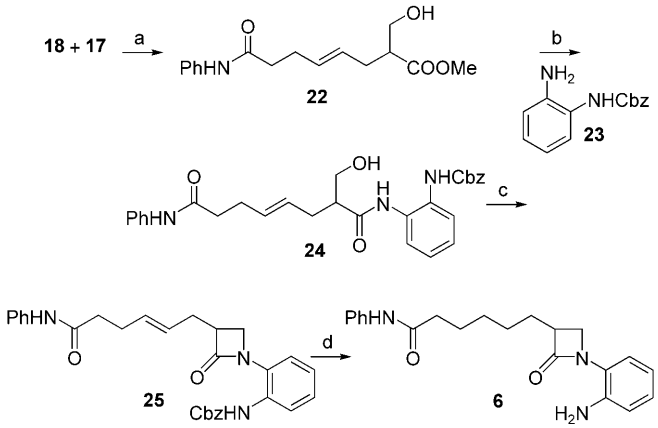

Scheme 5. *Reagents and conditions*: a) Grubbs II (5 mol%), CH_2Cl_2, reflux; b) LiHMDSA, THF −78 °C→−20 °C; c) DIAD, Ph_3P, THF, RT; d) H_2, Pd-C, THF/MeOH.

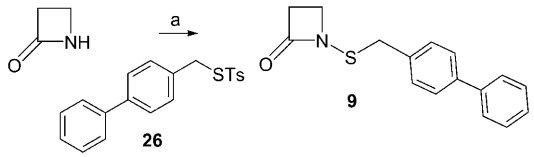

Scheme 6. *Reagents and conditions*: a) LiHMDSA, THF −78 °C.

HDAC isoforms inhibition assay

β-Lactams **1**–**9** were evaluated for their in vitro inhibitory activity against the 11 human HDACs isoforms to gain a complete profile on HDAC-isoform potency. The inhibitory activities were determined using a fluorescence-based assay with a fluorogenic peptide as the substrate (p53 379–382, ArgHisLysLys(Ac)). Trichostatin A (TSA) was used as the reference compound.[27a–c]

Separation of the stereoisomers of compounds **1**–**3**, **5** and **7**–**8** allowed single stereoisomers to be tested in the inhibition assay. The stereochemical configurations depicted in the structures (see Table 1) were tentatively attributed on the basis of the molecular modeling (see section entitled Computational Analysis).

Compounds **1**–**9** showed an unexpected isoform selectivity, with significant activity mainly against HDAC6 and HDAC8 (Table 1) and a lack of activity against other HDACs ($IC_{50} > 1000$ in all cases). Table 1 reports the IC_{50} data obtained against human HDAC6 and HDAC8 for the β-lactams tested.

Overall, the isoform selectivity did not change with modifications to the cap or linker moieties. However, the selectivity changed dramatically in response to modification on the substituent of the nitrogen atom of the β-lactam ring. The presence of an *N*-thiomethyl group increased the potency of these compounds against HDAC8. The most active compound was **1b** with an IC_{50} value of 4.53 μM. Compounds containing the *N*-phenylamide cap group were slightly more potent than those containing the *p*-phenyl group (cf. **3b** vs **8b**). The *E* or *Z* geometry of the double bond in the linker had no influence on the potency of the compounds. The position of the *N*-phenylamide side chain on the azetidinone ring (C3 or C4) slightly affected the activity; the side chain on the C4 position was a little more effective (cf. **1a**–**b** vs **3a**–**b**). Furthermore, the individual enantiomers had different inhibitory potencies against HDAC8 (cf. **3d** vs **3c**).

As opposed to the *N*-thiomethyl-azetidinones, the *N*-H or *N*-OH derivatives showed no activity against HDAC8, but some potency toward HDAC6; this is particularly apparent when **2a**–**b** and **3a**–**b** are compared. The presence of a C=C bond in the side chain had no influence on HDAC6 inhibition (see **2a**–**b** vs **4**). The *N*-*o*-aminophenyl group destroyed the activity against HDAC6 or HDAC8. The azetidinone **9**, with no side chains but with an *N*-thio-*p*-phenyl group, confirmed the effectiveness of a sulfur atom for increased HDAC8 activity, however, isoform selectivity was lost.

Computational analysis

In order to explain the selectivity of the *N*-thiomethyl-β-lactam derivatives **1a**–**b**, **3a**–**d**, and **8a**–**b** against the HDAC8 isoform, we performed a comparative structural study using three isoforms, HDAC2, HDAC7, and HDAC8, representative of class I and class II HDACs.

We speculated that the selectivity would be located within the active pocket in the channel and Zn-binding regions. The amino acids in these regions are highly conserved between class I and II HDACs, nevertheless, we turned our attention on two amino acids, Trp 141 and Met 274, that are specific to HDAC8 (Table 2). The interaction of *N*-thiomethyl-azetidin-2-one derivatives against class I and II HDACs were then evaluated using HDAC2, HDAC7, and HDAC8 isoforms as HDAC10 and -11, bearing unusual combinations of amino acids, are not reliable.

First, we calculated the geometry and energy of the Zn^{2+} in complex with the 1-methylsulfanyl-azetidin-2-one (*N*-thiomethyl-azetidin-2-one) unsubstituted at the C3 and C4 positions of the ring; a bidentate coordination geometry was found where distances between the Zn^{2+} ion and coordinating atoms (O and S) were 1.84 Å and 2.45 Å, respectively. This geometry was used as a starting point to superimpose the 1-methylsulfanyl-azetidin-2-one on the hydroxamic acid moiety of the inhibitors co-crystallized with the HDACs using the crystal structure of HDAC7 (PDB code: 3C0Z) and HADC8 (PDB code: 1T67)[15] and an in-house 3D structural model of HDAC2. In the active site, the Zn^{2+} coordination geometry is a square-based pyramid where the inhibitor and two aspartic acids form the base of the pyramid and a histidine is the vertex. After minimization, the 1-methylsulfanyl-azetidin-2-one loses bidentate coordination geometry in all the complexes because of unfavorable steric contacts with two conserved glycine residues (304 and 151 in HDAC8) with the methyl group and CH_2 on the C4 position of the azetidinone ring, respectively. We decided to use the model 1-methylsulfanyl-azetidin-2-one as a monodentate ligand, adding a water molecule as the fifth zinc coordinating group according to crystal structure of substrate–HDAC8 complex.[28a]

Using the *N*-thiomethyl-azetidinone **3c** as a representative ligand of the series in the configuration (*R*) of the C-3 position

Table 1. HDAC isoform selectivity profile of β-lactams **1**–**9**.[a]

Compd	Structure[b]	HDAC6 [μM]	HDAC8 [μM]	Compd	Structure[b]	HDAC6 [μM]	HDAC8 [μM]
TSA	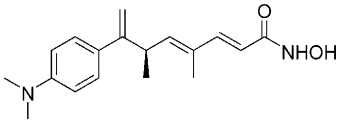	0.00042	0.089	**2a**	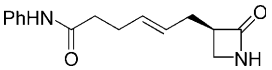	132.0	>1000
3a	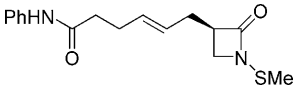	>1000	34.3	**2b**	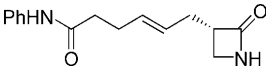	64.1	>1000
3b	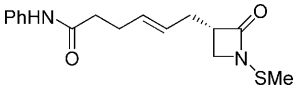	>1000	11.6	**2c**	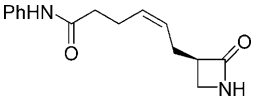	76.0	>1000
3c	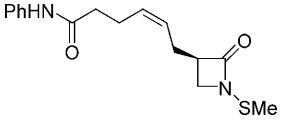	>1000	33.1	**2d**	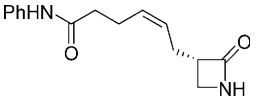	90.0	>1000
3d	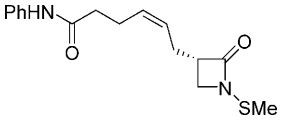	>1000	9.56	**5a**	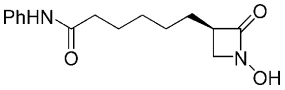	132	>1000
1a	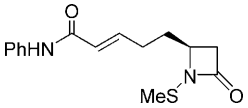	>1000	10.1	**5b**	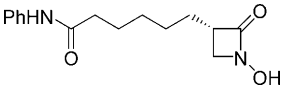	174	>1000
1b	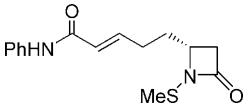	>1000	4.5	**7a**	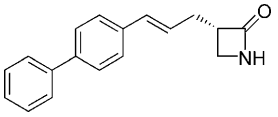	93.3	>1000
8a	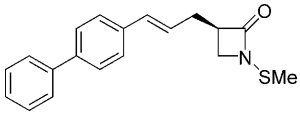	138	47.1	**7b**	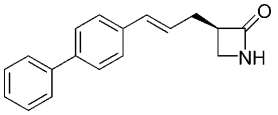	>1000	>1000
8b	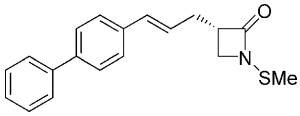	>1000	30.9	**4**	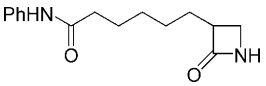	74.5	>1000
9	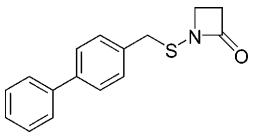	32.2	24.7	**6**	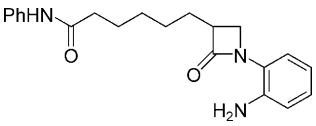	>1000	>1000

[a] See Experimental Section for assay conditions. Trichostatin A (TSA) was used as a reference compound. [b] Absolute configurations depicted are tentatively assigned on the basis of computational analysis (see text for details).

Table 2. Amino acid differences between HDAC8 and the other HDAC isoforms.

	Amino acid	Class I	Class II	Class IV
Zn-binding region	Trp 141	HDAC8	–	–
	Leu[a]	HDAC1–3	–	–
	Pro[a]	–	HDAC4–7, 9 & 10	–
	Phe 141	–	–	HDAC11
Channel region	Met 274	HDAC8	–	–
	Leu[a]	HDAC1–3	HDAC4–7 & 9	HDAC11
	Glu 272	–	HDAC10	–

[a] Numeration is variable in dependence of different HDAC isoforms.

of the ring, we performed molecular dynamic calculations of **3c**–H_2O–HDAC2, -7 and -8 complexes, to better characterize the interaction geometry. Molecular dynamics simulations were performed, and 100 structures for each complex were sampled and minimized. We calculated the mean distance between the Zn^{2+} ion and the coordinating heteroatom of the ligand, the mean number of contacts calculated between *N*-thiomethyl-azetidin-2-one ring and each nonconserved amino acid in the zinc-binding region (Leu 140, Pro 667, Trp 141), the mean number of contacts calculated between **3c** and each nonconserved amino acid in the linker region (Leu 272, Leu 810, Met 274), the mean number of contacts between **3c** and

amino acids in a range of 5 Å from the inhibitor, and $\Delta G_{binding}$ of **3c** for each HDAC. Table 3 shows the molecular dynamic simulation results; superimpositions of HDAC2/HDAC8 and HDAC7/HDAC8 minima are shown in Figure 3a and b.

Table 3. Mean distances and contacts from dynamics, and $\Delta G_{binding}$ values.

Isoform	Bond distance Zn–O/S [Å]	Good contacts Zn-binding-Leu/Pro/Trp	linker-Leu/Met	Total	$\Delta G_{binding}$[a] [kJ mol^{-1}]
HDAC2	2.64 (O)	0.1	11.0	222.4	−67.85
HDAC7	3.50 (S)	2.8	10.7	192.2	−99.26
HDAC8	2.23 (O)	16.1	12.5	255.4	−139.91

[a] Calculated from energy-minimized complexes.

The HDAC2 complex shows a more accessible space in the zinc-binding region compared with HDAC8,[28b] and as such can accommodate a larger ZBG, however, in this case the S-Me group of *N*-thiomethyl-azetidin-2-one is too small and does not interact with Leu 140. A good number of interactions are found between **3c** and Leu 272 in the linker region, however, these interactions are inferior than those with Met 242 in HDAC8. Moreover, azetidin-2-one makes poor contacts with Gly 150 and Phe 151.

Analyzing the HDAC8 complex, we noted that **3c** maximizes the numbers of contacts in both regions without bad interactions and anchors the cap group to the external region of the enzyme via a H bond with Phe 207 (residue not shown in the figures for clarity). Both complexes maintain a Zn^{2+}–carbonyl interaction similar to the natural substrate (acetylated lysine).[28a] Conversely, the S-Me group of 1-methylsulfanyl-azetidin-2-one makes bad contacts with Pro 667 in HDAC7, and during the simulation **3c** moves until the S atom is in the correct position to coordinate with the Zn^{2+} ion. However, the S-Me group still interacts with Pro 667. The total numbers of contact between **3c** and HDAC7 decreases due to the more external binding orientation in comparison with other complexes.

By measuring the $\Delta G_{binding}$ of the three minima, we can see that the order of stability of **3c**–HDACs complexes is HDAC8 > HDAC7 > HDAC2, in good accordance with the isoform selectivity found in the in vitro tests. Considering the monodentate coordination geometry of this ligand with respect to a bidentate one, the lower activities of these new β-lactam ligands compared with SAHA or TSA can be justified.

Subsequently, we used the refined **3c**–HDAC8 complex to dock compounds **1a**, **1b**, **3a**, **3b**, **3c**, **3d**, **8a**, and **8b** and to compare them in terms of $\Delta G_{binding}$. As shown in Figure 4a, all the inhibitors adopted the same orientation as **3c** with the carbonyl coordinating to the zinc ion, thus confirming *N*-thiomethyl-azetidinone as a valuable zinc-binding group (ZBG).

We determined that each enantiomeric couple oriented the *N*-thiomethyl-azetidin-2-one ring with respect to the Zn^{2+}–carbonyl coordination bond: *N*-thiomethyl-azetidin-2-one interacts with Trp 141 via the sulfur atom when the orientation of the side chain is "down", and via the methyl group when it is "up" (Figure 4b). Compounds with "down" stereochemistry have G_{score} and $\Delta G_{binding}$ values higher than the "up" stereoisomers, and we speculated that for each enantiomeric couple a "down" configuration could be assigned to the most active compound: $\Delta\Delta G_{binding}$ **1b**–**1a** = −18 kJ mol^{-1}; **3b**–**3a** = −12 kJ mol^{-1}; **3d**–**3c** = −21 kJ mol^{-1}; **8b**–**8a** = −38 kJ mol^{-1}.

Conclusions

The results reported here on the development of selective and potent HDAC inhibitors should shed light onto the connections between HDAC isoforms and pathophysiology, such as inflammation, cancer or immunological diseases, and validate the targeting of specific HDACs for the improved treatment of certain disease conditions with reduced side effects.

Monocyclic azetidin-2-ones, specifically designed using the HDAC inhibitor pharmacophore model, were shown to selectively inhibit HDAC6 and HDAC8. We were able to manipulate the isoform selectivity by modifying the substituent on the nitrogen atom of the β-lactam ring. In particular, *N*-thiomethyl-azetidin-2-ones showed a stringent isoform selectivity towards

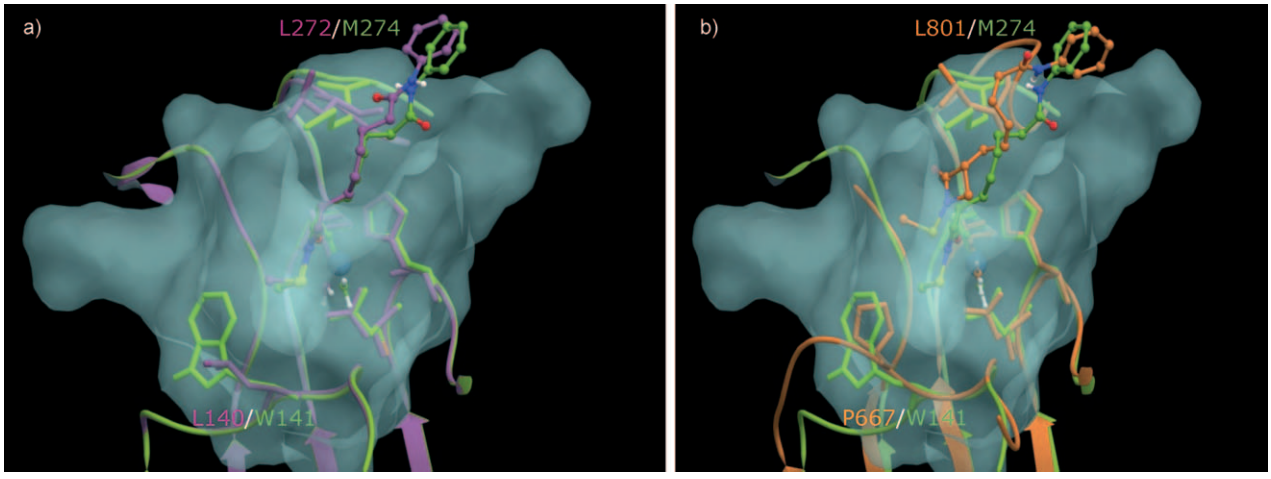

Figure 3. a) **3c**–HDAC2/8 complexes (purple and green, respectively; ball and stick representation); b) **3c**–HDAC7/8 complexes (orange and green, respectively; ball and stick representation).

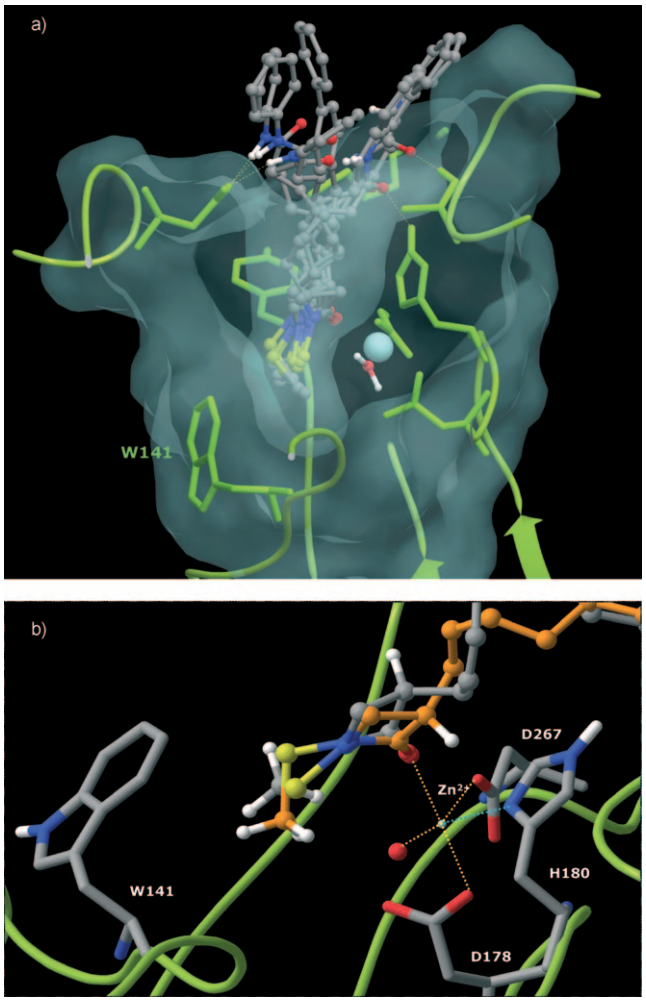

Figure 4. a) Four enantiomeric couples of compounds (ball and stick representation) in complex with HDAC8 (green); b) comparison of docking pose for enantiomers **3c** (grey) and **3d** (orange).

HDAC8 with activities in the micromolar range. Molecular modeling provided a structural explanation for the isoform selectivity and for the differences in activities between enantiomers, and also gave support to the tentatively assigned absolute configurations of the isolated stereoisomers.

Furthermore, our findings have validated the β-lactam ring as a novel zinc-binding group,[29] which is worthy of further investigation and optimization in the design of new HDAC8-selective inhibitors.

Experimental Section

Chemical synthesis

All reactions were performed under N_2. Commercial reagents were used as received without additional purification. Anhydrous solvents (CH_3CN, CH_2Cl_2, THF) were obtained commercially. ^1H and ^{13}C NMR values were recorded on an INOVA 400, Varian INOVA 300 or a GEMINI 200 instrument with a 5 mm probe. All chemical shifts (δ) are quoted in ppm relative to residual solvent signals. Coupling constants (J) are given in Hz. FT-IR were recorded on a Nicolet 380; samples were prepared as films between NaCl plates and the wavenumbers are reported in cm^{-1}. TLC was carried out using Merck 60 F_{254} plates and column chromatography was performed on Merck silica gel 200–300 mesh. GC-MS: Agilent Technologies, column HP5 5% Ph-Me. Silicon MS: Agilent Technologies MSD1100 single-quadrupole mass spectrometer, EI voltage 70 eV, gradient from 50→280 °C over 30 min. HPLC-MS, HPLC: Agilent Technologies HP1100, column ZOBRAX-Eclipse XDB-C8 Agilent Technologies, mobile phase: H_2O/CH_3CN, gradient from 30→80% of CH_3CN in 8 min, 80% of CH_3CN until 25 min, 0.4 mL min^{-1}; MS: Agilent Technologies MSD1100 single-quadrupole mass spectrometer, full-scan mode from m/z 50→2600, scan time 0.1 s in positive ion mode, ESI spray voltage 4500 V, nitrogen gas 35 psi, drying gas flow 11.5 mL min^{-1}, fragmentor voltage 20 V. HRMS analysis were recorded on a MAT 95 XP Thermo Finnigan.

β-Lactam **10** was prepared from commercially available 4-acetoxy-azetidin-2-one following a known procedure.[30] Product **11** is known,[31] but was prepared following a modified procedure. Product **13** was prepared following the procedure reported in Reference [32]. Product **14** was prepared following the procedure reported in Reference [33]. Product **15** is known.[34] Product **17** was prepared following the procedure reported in Reference [35]. Product **18** is known.[36] Compound **23** is known,[37] but was prepared following the procedure reported in Reference [38]. Further details on the preparation of compounds **11**, **14**, and **15** can be found in the Supporting Information, as can full spectral data on intermediate compounds.

4-But-3-enyl-1-methylsulfanyl-azetidin-2-one (12): A solution of **11** (223 mg, 2.0 mmol) in THF (20 mL) at −78 °C was first treated with LiHMDSA (2.2 mmol, 1 M in THF) and then *S*-methyl methanethiosulfonate (0.5 mL, 5 mmol). The reaction was allowed to reach RT and stirred for 3 h before being quenched with aq NH_4Cl and extracted with EtOAc. The organic extracts were dried (Na_2SO_4), filtered and concentrated in vacuo. Flash chromatography (cyclohexane/EtOAc, 50:50) gave **12** as a yellow oil (134 mg, 94% yield): R_f = 0.50 (cyclohexane/EtOAc, 50:50).

(*E*)-5-(1-methylsulfanyl-4-oxo-azetidin-2-yl)pent-2-enoic acid phenylamide (1): A solution of **12** (94 mg, 0.55 mmol) and *N*-phenylacrylamide **13** (162 mg, 1.1 mmol) in CH_2Cl_2 (2.8 mL) was degassed using freeze-pump-thaw procedure and treated with Grubbs 2nd-generation catalyst (23 mg, 5 mol%). The reaction was monitored by TLC. After 14 h at reflux, the catalyst was removed by filtration and the filtrate was concentrated in vacuo. Flash chromatography (cyclohexane/EtOAc, 90:10) gave **1** as a colorless oil (81 mg, 51%); R_f = 0.47 (cyclohexane/EtOAc, 50:50); ^1H NMR (200 MHz, $CDCl_3$, 22 °C): δ = 1.58–1.74 (m, 1H), 2.01–2.18 (m, 1H), 2.26–2.37 (m, 2H), 2.41 (s, 3H), 2.66 (dd, J = 3.0, J = 15.0 Hz, 1H), 3.10 (dd, J = 5.0, J = 15.0 Hz, 1H), 3.62–3.74 (m, 1H), 6.06 (d, J = 15.0 Hz, 1H), 6.87–7.06 (m, 1H), 7.10–7.13 (m, 1H), 7.27–7.35 (m, 2H), 7.58–7.62 (m, 2H), 8.00 ppm (br s, 1H); ^{13}C NMR (100 MHz, $CDCl_3$, 24 °C): δ = 22.7, 28.0, 31.8, 43.6, 55.0, 119.9, 124.4, 125.1, 129.0, 129.1, 138.0, 144.0, 170.3; IR (film): $\tilde{\nu}$ = 3312, 2922, 1752, 1676 cm^{-1}; HPLC-MS (ESI): R_t = 5.9 min, m/z: 291 $[M+H]^+$, 313 $[M+Na]^+$, 603 $[2M+Na]^+$; HRMS (EI): m/z $[M]^+$ calcd for $C_{15}H_{18}N_2O_2S$: 290.1089, found: 290.1089.

Separation of the two enantiomers using semi-preparative HPLC (Daicel Chiralcel AD, 0.46 cm ∅ ×25 cm; 0.5 mL min^{-1}; *n*-hexane/*i*PrOH, 75:25) gave: **1a** (R_t = 20.4 min); **1b** (R_t = 24.3 min).

(*E*)-6-(2-oxo-azetidin-3-yl)hex-4-enoic acid phenylamide (2): A solution of **15** (76 mg, 0.7 mmol) and *N*-phenylpent-4-enamide **17** (257 mg, 1.5 mmol) in CH_2Cl_2 (4 mL) was degassed using the freeze-pump-thaw procedure and treated with Grubbs 2nd-genera-

tion catalyst (29 mg, 5 mol%). After 12 h at reflux, the reaction was stopped by removal of the catalyst and the filtrate was concentrated in vacuo. Flash chromatography (cyclohexane/EtOAc, 60:40) gave **2** as a colorless oil (101 mg, 58%); $R_f = 0.25$ (cyclohexane/EtOAc, 40:60); ^{1}H NMR (300 MHz, [D$_6$]acetone, 22 °C): $\delta = 2.22$–2.45 (m, 6H), 2.93 (dd, $J = 2.4$, $J = 5.4$ Hz, 1H), 3.14–3.22 (m, 1H), 3.27 (dd, $J = 5.1$, $J = 5.4$ Hz, 1H), 5.50–5.66 (m, 2H), 6.80 (br s, 1H), 7.0–7.05 (m, 1H), 7.24–7.30 (m, 2H), 7.64–7.67 (m, 2H), 9.12 ppm (br s, 1H); ^{13}C NMR (75 MHz, [D$_6$]acetone, 24 °C): $\delta = 29.3$, 32.5, 37.8, 41.1, 51.9, 120.1, 124.0, 128.1, 130.0, 132.1, 140.6, 170.9, 171.4 ppm; IR (film): $\tilde{\nu} = 3301$, 2923, 1736, 1664 cm^{-1}; HPLC-MS (ESI): $R_t = 2.2$ min, *m/z*: 259 $[M+H]^+$, 539 $[2M+Na]^+$; HRMS (EI): *m/z* $[M]^+$ calcd for $C_{15}H_{18}N_2O_2$: 258.1368, found: 258.1371.

On selected fractions enriched with the *Z* isomer, separation of the four stereoisomers using semi-preparative HPLC (Daicel Chiralcel OD, 0.46 cm ∅ ×25 cm; 0.5 mL min^{-1}; *n*-hexane/*i*PrOH, 85:15) gave: **2c**(*Z*) ($R_t = 36.6$ min); **2d**(*Z*) ($R_t = 38.9$ min); **2a**(*E*) ($R_t = 40.8$ min); **2b**(*E*) ($R_t = 44.0$ min).

6-(2-oxo-azetidin-3-yl)hexanoic acid phenylamide (4): Pd-C (10% *w/w*) (2.1 mg, 0.2 equiv) was added to a solution of **2** (10.5 mg, 0.04 mmol) in THF (1.5 mL) and MeOH (1.5 mL) and the mixture was stirred under H_2 (8 bar). After full conversion, the reaction mixture was filtered and concentrated in vacuo to afford **4** as a colorless oil (10 mg, quantitative yield); $R_f = 0.20$ (cyclohexane/EtOAc, 30:70); ^{1}H NMR (300 MHz, [D$_6$]acetone, 22 °C): $\delta = 1.33$–1.50 (m, 4H), 1.59–1.74 (m, 4H), 2.36 (t, $J = 7.2$ Hz, 2H), 2.94 (dd, $J = 2.7$, $J = 5.4$ Hz, 1H), 3.11–3.19 (m, 1H), 3.35 (dd, $J = 5.4$, $J = 5.4$ Hz, 1H), 6.83 (br s, 1H), 6.99–7.05 (m, 1H), 7.23–7.30 (m, 2H), 7.65–7.68 (m, 2H), 9.13 ppm (br s, 1H); ^{13}C NMR (50 MHz, [D$_6$]acetone, 24 °C): $\delta = 26.2$, 27.6, 29.8, 29.9, 37.7, 42.0, 52.4,120.1, 124.0, 129.5, 140.7, 171.5, 172.0 ppm; IR (film): $\tilde{\nu} = 3301$, 2960, 2926, 1736, 1664 cm^{-1}; HPLC-MS (ESI): $R_t = 7.0$ min, *m/z*: 261 $[M+H]^+$, 543 $[2M+Na]^+$; HRMS (EI): *m/z* $[M]^+$ calcd for $C_{15}H_{20}N_2O_2$: 260.1525, found: 260.1527.

3-Allyl-1-methylsulfanyl-azetidin-2-one (16): A solution of **15** (80 mg, 0.7 mmol) in THF (4 mL) at −78 °C was first treated with LiHMDSA (0.8 mmol, 1 M in THF) and then *S*-methyl methanetiosulfonate (0.2 mL, 1.8 mmol). The solution was warmed to RT and stirred for 3 h. The reaction was quenched with aq NH_4Cl and extracted with EtOAc. The organic extracts were dried (Na_2SO_4), filtered and concentrated in vacuo. Flash chromatography (cyclohexane/EtOAc, 80:20) gave **16** as a pale yellow oil (70 mg, 62% yield); $R_f = 0.75$ (cyclohexane/EtOAc, 50:50).

(*E*)-6-(1-methylsulfanyl-2-oxo-azetidin-3-yl)hex-4-enoic acid phenylamide (3): A solution of **16** (63 mg, 0.4 mmol) and *N*-phenylpent-4-enamide (176 mg, 1 mmol) in CH_2Cl_2 (2 mL) was degassed using the freeze-pump-thaw procedure and treated with Grubbs 2nd-generation catalyst (17 mg, 5 mol%). After 4 h at reflux, the reaction was filtered to remove the catalyst, and the filtrate was concentrated in vacuo. Flash chromatography (cyclohexane/EtOAc, 70:30) gave **3** as a colorless oil (45 mg, 37%); $R_f = 0.35$ (cyclohexane/EtOAc, 50:50); ^{1}H NMR (200 MHz, CD_3CN, 22 °C): $\delta = 2.22$–2.46 (m, 6H), 2.37 (s, 3H), 3.10 (dd, $J = 3.0$ Hz, $J = 5.4$ Hz, 1H), 3.23–3.33 (m, 1H), 3.40 (dd, $J = 5.2$, $J = 5.4$ Hz, 1H), 5.40–5.64 (m, 2H), 7.03–7.10 (m, 1H), 7.26–7.34 (m, 2H), 7.53–7.58 (m, 2H), 8.28 ppm (br s, 1H); ^{13}C NMR (50 MHz, CD_3CN, 24 °C): $\delta = 21.4$, 28.5, 31.3, 36.9, 48.5, 51.3,119.8, 123.9, 126.8, 129.1, 132.1, 139.5, 171.2, 173.4 ppm; IR (film): $\tilde{\nu} = 3320$, 2922, 1736, 1655 cm^{-1}; HPLC-MS (ESI): $R_t = 7.1$ min, *m/z*: 305 $[M+H]^+$, 327 $[M+Na]^+$, 631 $[2M+Na]^+$; HRMS (EI): *m/z* $[M]^+$ calcd for $C_{16}H_{20}N_2O_2S$: 304.1245, found: 304.1244.

On selected fractions enriched with the *Z* isomer, separation of the four stereoisomers using semi-preparative HPLC (Daicel Chiralcel OD, 0.46 cm ∅ ×25 cm; 0.5 mL min^{-1}; *n*-hexane/*i*PrOH, 82:18→70:30 over 25 min) gave: **3c**(*Z*) ($R_t = 20.1$ min); **3d**(*Z*) ($R_t = 22.6$ min); **3a**(*E*) ($R_t = 29.0$ min); **3b**(*E*) ($R_t = 34.0$ min).

3-(3-Biphenyl-4-yl-allyl)azetidin-2-one (7): A solution of **15** (22 mg, 0.2 mmol) and 4-phenyl styrene (90 mg, 0.5 mmol) in CH_2Cl_2 (1 mL) was degassed using the freeze-pump-thaw procedure and treated with Grubbs 2nd-generation catalyst (8.5 mg, 5 mol%). After 14 h at reflux, the reaction was filtered to remove the catalyst, and the filtrate was concentrated in vacuo. Flash chromatography (cyclohexane/EtOAc, 70:30) gave **7** as a colorless oil (20 mg, 38%); $R_f = 0.34$ (cyclohexane/EtOAc, 50:50); ^{1}H NMR (300 MHz, $CDCl_3$, 22 °C): $\delta = 2.58$–2.60 (m, 1H), 2.70–2.79 (m, 1H), 3.08–3.16 (m, 1H), 3.40–3.50 (m, 2H), 5.66 (br s, 1H), 6.28 (dt, $J = 6.9$, $J = 15.6$ Hz, 1H), 6.52 (d, $J = 15.6$ Hz, 1H), 7.27–7.64 ppm (m, 9H); ^{13}C NMR (75 MHz, $CDCl_3$, 24 °C): $\delta = 31.9$, 41.0, 51.0, 125.9, 126.6, 126.9, 127.2, 127.3, 128.8, 131.9, 136.1, 140.1, 140.7, 170.7 ppm; IR (Nujol): $\tilde{\nu} = 3190$, 1736, 1704 cm^{-1}; HPLC-MS (ESI): $R_t = 9.1$ min, *m/z*: 264 $[M+H]^+$, 281 $[M+H_2O]^+$, 527 $[2M+H]^+$, 549 $[2M+Na]^+$; HRMS (EI): *m/z* $[M]^+$ calcd for $C_{18}H_{17}NO$: 263.1310, found: 263.1311.

Separation of the two enantiomers using semi-preparative HPLC (Daicel Chiralcel OD, 0.46 cm ∅ ×25 cm; 0.5 mL min^{-1}; *n*-hexane/*i*PrOH, 88:12) gave: **7a** ($R_t = 28.3$ min); **7b** ($R_t = 31.8$ min).

3-(3-Biphenyl-4-yl-allyl)-1-methylsulfanyl-azetidin-2-one (8): A solution of **16** (40 mg, 0.3 mmol) and 4-phenyl styrene (114 mg, 0.6 mmol) in CH_2Cl_2 (2 mL) was degassed using the freeze-pump-thaw procedure and treated with Grubbs 2nd-generation catalyst (8.5 mg, 5 mol%). After 14 h at reflux, the reaction was filtered to remove the catalyst, and the filtrate was concentrated in vacuo. Flash chromatography (cyclohexane/EtOAc, 90:10) gave **8** as a colorless oil (33 mg, 43%); $R_f = 0.20$ (cyclohexane/EtOAc, 80:20); ^{1}H NMR (300 MHz, $CDCl_3$, 22 °C): $\delta = 2.45$ (s, 3H), 2.56–2.67 (m, 1H), 2.71–2.79 (m, 1H), 3.28 (dd, $J = 2.7$ Hz, $J = 5.7$ Hz, 1H), 3.48–3.55 (m, 1H), 3.59 (dd, $J = 5.1$, $J = 5.7$ Hz, 1H), 6.26 (dt, $J = 7.2$, $J = 15.6$ Hz, 1H), 6.54 (d, $J = 15.6$ Hz, 1H), 7.29–7.68 ppm (m, 9H); ^{13}C NMR (50 MHz, $CDCl_3$, 24 °C): $\delta = 21.9$, 31.8, 48.6, 51.1, 125.1, 126.5, 126.8, 127.2, 127.3, 128.7, 132.3, 135.8, 140.2, 140.6, 173.2 ppm; IR (film): $\tilde{\nu} = 2920$, 2850, 1750 cm^{-1}; HPLC-MS (ESI): $R_t = 11.1$ min, *m/z*: 310 $[M+H]^+$, 327 $[M+H_2O]^+$, 619 $[2M+H]^+$, 641 $[2M+Na]^+$; HRMS (EI): *m/z* $[M]^+$ calcd for $C_{19}H_{19}NOS$: 309.1187, found: 309.1186.

Separation of the two enantiomers using semi-preparative HPLC (Daicel Chiralcel OD, 0.46 cm ∅ ×25 cm; 0.5 mL min^{-1}; *n*-hexane/*i*PrOH, 58:42) gave: **8a** ($R_t = 15.9$ min); **8b** ($R_t = 19.0$ min).

2-Hydroxymethylpent-4-enoic acid benzyloxyamide (19): *n*BuLi (2.20 mmol, 1.6 M in hexane) was added dropwise to an ice-cold solution of hexamethyldisilylamine (417 μL, 2.00 mmol) in THF (2 mL). The ice bath was removed and the reaction was stirred at RT for 30 min. The mixture was added dropwise via cannula to a suspension of $BnONH_2$·HCl (64 mg, 0.40 mmol) in THF (5 mL) at −78 °C. Finally, a solution of compound **18** (50 mg, 0.35 mmol) in THF (2 mL) was added dropwise to the mixture at −78 °C. The reaction was monitored by TLC until disappearance of the starting material. The reaction mixture was quenched with aq NH_4Cl (10 mL), extracted with EtOAc (3×8 mL), the organic layer was dried (Na_2SO_4), filtered and concentrated in vacuo. Flash chromatography (cyclohexane/EtOAc, 50:50) gave **19** as a pale yellow oil (40 mg, 48%); $R_f = 0.25$ (cyclohexane/EtOAc, 20:80).

3-Allyl-1-benzyloxy-azetidin-2-one (20): A solution of **19** (40 mg, 0.17 mmol) in THF (10 mL) was treated with PPh_3 (50 mg, 0.19 mmol) and DIAD (37 μL, 0.19 mmol) and stirred at RT (moni-

tored by TLC). After 4.5 h the reaction was concentrated in vacuo. Flash chromatography (cyclohexane/EtOAc, 90:10) gave **20** as a pale yellow oil (36 mg, 96%); $R_f = 0.60$ (cyclohexane/EtOAc, 70:30).

6-(1-Benzyloxy-2-oxo-azetidin-3-yl)hex-4-enoic acid phenylamide (21): A solution of **20** (26 mg, 0.12 mmol) and *N*-phenylpent-4-enamide (52 mg, 0.30 mmol) in CH_2Cl_2 (0.8 mL) was degassed using the freeze-pump-thaw procedure and treated with Grubbs 2nd-generation catalyst (5 mg, 5 mol%). The reaction mixture was refluxed and monitored by TLC. After 20 h at reflux, the reaction was cooled, filtered and concentrated in vacuo. Flash chromatography (cyclohexane/EtOAc, 80:20) gave **21** as a colorless oil (20 mg, 44%); $R_f = 0.30$ (cyclohexane/EtOAc, 70:30).

6-(1-Hydroxy-2-oxo-azetidin-3-yl)hexanoic acid phenylamide (5): Pd-C (10% *w/w*) (3.0 mg, 20%) was added to a solution of **21** (30.0 mg, 0.08 mmol) in THF and MeOH (2.5 mL, 4:1) and the mixture was stirred under H_2 (1 bar). The reaction was monitored by TLC. After completion, the reaction was filtered and concentrated in vacuo. Flash chromatography (cyclohexane/EtOAc, 70:30) gave **5** as a colorless oil (22 mg, quantitative yield); $R_f = 0.40$ (cyclohexane/EtOAc, 50:50); ^{1}H NMR (300 MHz, [D$_6$]acetone, 22 °C): $\delta = 1.27$–1.72 (m, 8H), 2.35 (t, 2H, $J = 7.5$ Hz), 2.83–2.88 (m, 1H), 3.17 (dd, 1H, $J = 2.4$ Hz, $J = 4.5$ Hz), 3.58 (dd, 1H, $J = 4.5$ Hz, $J = 5.1$ Hz), 6.98–7.04 (m, 1H), 7.23–7.29 (m, 2H), 7.63–7.66 (m, 2H), 9.02 (br s, 1H), 9.09 ppm (br s, 1H); ^{13}C NMR (75 MHz, [D$_6$]acetone, 24 °C): $\delta = 26.0$, 27.5, 27.7, 29.7, 37.5, 45.6, 52.6, 119.9, 123.8, 129.4, 140.5, 167.4, 171.9 ppm; IR (film): $\tilde{\nu} = 3450$, 1740, 1710, 1660 cm^{-1}; HPLC-MS (ESI): $R_t = 4.8$ min, *m/z*: 277 $[M+H]^+$, 575 $[2M+Na]^+$; HRMS (EI): *m/z* $[M]^+$ calcd for $C_{15}H_{20}N_2O_3$: 276.1474, found: 276.1474.

Separation of the two enantiomers using semi-preparative HPLC (Daicel Chiralpak IC, 0.46 cm ∅ × 25 cm; 0.6 mL min^{-1}; *n*-hexane/*i*PrOH, 70:30) gave: **5a** ($R_t = 20.5$ min); **5b** ($R_t = 21.4$ min).

2-Hydroxymethyl-7-phenylcarbamoylhept-4-enoic acid methyl ester (22): A solution of **18** (60 mg, 0.42 mmol) and *N*-phenylpent-4-enamide (182 mg, 1.04 mmol) in CH_2Cl_2 (2 mL) was degassed using the freeze-pump-thaw procedure and treated with Grubbs 2nd-generation catalyst (18 mg, 5 mol%). The mixture was refluxed and monitored by TLC until disappearance of the starting material. The reaction was cooled, filtered to remove the catalyst, and concentrated in vacuo. Flash chromatography (cyclohexane/EtOAc, 75:25) gave **22** as a colorless oil (58 mg, 47%); $R_f = 0.30$ (cyclohexane/EtOAc, 60:40).

[2-(2-Hydroxymethyl-7-phenylcarbamoylhept-4-enoylamino)phenyl]carbamic acid benzyl ester (24): *n*BuLi (0.75 mmol, 1.6 M in hexane) was added dropwise to an ice-cold solution of hexamethyldisilylamine (140 μL, 0.67 mmol) in THF (1 mL). The ice bath was removed and the reaction was stirred at RT for 30 min. The mixture was added dropwise via cannula to a suspension of (2-aminophenyl)carbamic acid benzyl ester (24 mg, 0.10 mmol) in THF (0.8 mL) at −78 °C. Finally, a solution of **22** (28 mg, 0.10 mmol) in THF (1.5 mL) was added dropwise to the mixture at −78 °C. The mixture was allowed to slowly reach RT and monitored by TLC until disappearance of the starting material. The reaction was quenched with aq NH_4Cl, extracted with EtOAc, and the organic extracts were dried (Na_2SO_4), filtered and concentrated in vacuo. Flash chromatography (cyclohexane/EtOAc, 50:50) gave **24** as a pale yellow oil (104 mg, 67%); $R_f = 0.35$ (cyclohexane/EtOAc, 30:70).

{2-[2-Oxo-3-(5-phenylcarbamoylpent-2-enyl)azetidin-1-yl]phenyl}carbamic acid benzyl ester (25): A solution of **24** (100 mg, 0.20 mmol) in THF (11 mL) was treated with PPh_3 (58 mg, 0.22 mmol) and DIAD (43 μL, 0.22 mmol) and stirred at RT (monitored by TLC). After full conversion, the mixture was concentrated in vacuo. Flash chromatography (cyclohexane/EtOAc, 50:50) gave **25** as a pale yellow oil (75 mg, 77%); $R_f = 0.70$ (cyclohexane/EtOAc, 30:70).

6-[1-(2-Aminophenyl)-2-oxo-azetidin-3-yl]hexanoic acid phenylamide (6): Pd-C (10% *w/w*) (14 mg, 20%) was added to a solution of **25** (63 mg, 0.13 mmol) in THF and MeOH (2.5 mL, 3:2) and the mixture was stirred under H_2 (1 bar). The reaction was monitored by TLC. After full conversion, the reaction mixture was filtered and concentrated in vacuo to afford the product as a colorless oil (45 mg, quantitative yield); $R_f = 0.48$ (cyclohexane/EtOAc, 30:70); ^{1}H NMR (300 MHz, $CDCl_3$, 22 °C): $\delta = 1.43$–1.93 (m, 8H), 2.37 (t, 2H, $J = 7.5$ Hz), 3.25 (m, 1H), 3.38 (dd, 1H, $J = 2.7$ Hz, $J = 5.7$ Hz), 3.78 (dd, 1H, $J = 5.7$ Hz, $J = 5.7$ Hz), 4.81(br s, 2H), 6.69–6.74 (m, 2H), 6.81–6.84 (m, 1H), 6.98–7.04 (m, 1H), 7.07–7.12 (m, 1H), 7.29–7.34 (m, 2H), 7.37 (br s, 1H), 7.51–7.54 ppm (m, 2H); ^{13}C NMR (75 MHz, $CDCl_3$, 24 °C): $\delta = 25.2$, 26.5, 28.6, 28.8, 37.4, 45.5, 46.4, 117.5, 118.0, 119.0, 119.7, 124.1, 125.4, 126.5, 128.9, 138.0, 139.2, 167.6, 171.2 ppm; IR (film): $\tilde{\nu} = 3450$, 3300, 1710, 1696, 1663 cm^{-1}; HPLC-MS (ESI): $R_t = 8.2$ min, *m/z*: 352 $[M+H]^+$, 374 $[M+Na]^+$, 725 $[2M+Na]^+$; HRMS (EI): *m/z* $[M]^+$ calcd for $C_{21}H_{25}N_3O_2$: 351.1947, found: 351.1945.

Toluene-4-thiosulfonic acid *S*-biphenyl-4-ylmethyl ester (26): 4-Phenylbenzyl chloride (101 mg, 0.5 mmol) was added to a solution of potassium thiotosylate (113 mg, 0.5 mmol) in DMF (2 mL). After 48 h, the reaction was quenched with aq HCl (0.1 M) and extracted with Et_2O, the organic extracts were dried (Na_2SO_4), filtered and concentrated in vacuo. Flash chromatography (cyclohexane/EtOAc, 90:10) gave **26** as a colorless oil (150 mg, 85% yield); $R_f = 0.40$ (cyclohexane/EtOAc, 90:10).

1-(Biphenyl-4-ylmethylsulfanyl)azetidin-2-one (9): A solution of azetidin-2-one (14 mg, 0.2 mmol) in THF (5 mL) at −78 °C was treated first with LiHMDSA (0.22 mmol, 1 M in THF) and then *S*-[(4-phenyl)benzyl]-4-methylbenzenesulfonothioate (90 mg, 0.25 mmol). The solution was allowed to warm to RT. After 2 h the reaction was cooled to 0 °C and quenched with aq NH_4Cl. The mixture was extracted with EtOAc, the organic extracts were dried (Na_2SO_4), filtered and concentrated in vacuo. Flash chromatography (cyclohexane/EtOAc, 80:20) gave **9** as a yellow oil (45 mg, 84% yield); $R_f = 0.44$ (cyclohexane/EtOAc, 80:20); ^{1}H NMR (300 MHz, $CDCl_3$, 22 °C): $\delta = 2.87$–2.95 (m, 4H), 3.94–3.99 (m, 2H), 7.28–7.56 ppm (m, 9H); ^{13}C NMR (75 MHz, $CDCl_3$, 24 °C): $\delta = 38.6$, 42.5, 44.3, 126.9, 127.3, 127.4, 128.8, 129.7, 135.1, 140.3, 140.5, 170.9 ppm; IR (film): $\tilde{\nu} = 3050$, 3000, 1757 cm^{-1}; HPLC-MS (ESI): $R_t = 9.5$ min, *m/z*: 270 $[M+H]^+$, 287 $[M+H_2O]^+$, 292 $[M+Na]^+$, 561 $[2M+Na]^+$; HRMS (EI): *m/z* $[M]^+$ calcd for $C_{16}H_{15}NOS$: 269.0874, found: 269.0873.

Biological assay

The enzyme inhibition assay was carried out as previously described.[27] Briefly, compounds were tested in 10-dose IC_{50} mode in duplicate with threefold serial dilutions starting at 50 μM against human HDAC enzymes (1–11). A fluorogenic peptide was used as the substrate, consisting of a fluorogenic moiety bound to a specific p53 fragment (residues 379–392, ArgHisLysLys(Ac)), which includes an ε-acetylated lysine side chain. Upon deacetylation of the substrate, the fluorophore was released giving rise to fluorescence, which was detected using a fluorimeter, and the IC_{50} values of the test compounds were determined by analyzing dose-response inhibition curves.

Computational analysis

Determination of the geometry of metal–ligand interaction: The zinc-binding group, represented by 1-methylsulfanyl-azetidin-2-one, was complexed to Zn^{2+} in a bidentate geometry. The conformation was minimized using semi-empirical PM3 method and then an ab initio Hartree–Fock 3-21G* single-point calculation was applied to determine the energy of the complex (SPARTAN'04; Wavefunction, Inc., http://www.wavefun.com).

Homology modeling of HDAC2 isoform: We built a 3D model of HDAC2 using HDAC8 as the main template (PDB code: 1T67) and HDLP as the template for L1 and L7 loops (PDB code: 1C3S). MS-344 was used as an internal ligand during the modeling phase (~10 Å from it) and as external ligand during the validation phase, obtaining an RMSD value of 1.0 between the co-crystallized and docked solution. Homology modeling was performed by Prime 1.5 (Schrödinger L.L.C, Portland, USA) and refinement using Macromodel (version 9.1; Schrödinger). Docking procedure was performed by Glide (version 4.0; Schrödinger).

Molecular dynamics and minimization: Molecular dynamics of each HDAC isoform (HDAC2, homology model; HDAC7, PDB code: 3C0Z; HDAC8, PDB code: 1T67) with the ligand **3c** was carried out at 300 K with time step of 1.5 fs. Amino acids side chains within a shell of 5 Å from the ligand were taken unconstrained, while the backbone was frozen; the Zn^{2+}–water distance was constrained to 2.0 ± 0.2 Å. The system was equilibrated for a period of 100 ps, followed by a production run of 1 ns, using Macromodel (version 9.1; Schrödinger). Then, 100 solutions were saved and minimized (TNCG; 2000 steps up to 0.01 gradient threshold). $\Delta G_{binding}$ was calculated using the MM-GBSA method, performed by Prime 1.5 (Schrödinger).

Docking procedure: Eight compounds, owing to three different series, were docked on HDAC8 using the refined complex with **3c**. Docking procedure was performed on Glide (version 4.0; Schrödinger), using SP protocol. Poses with the best G score were selected and compared in terms of $\Delta G_{binding}$.

Acknowledgements

We thank Dr. M. Gobbini for quantum-chemical calculations and Mr. A. Garelli for HPLC technical assistance. Prof. G. Cainelli is greatly acknowledged for his enthusiasm and support.

Keywords: azetidinones · heterocycles · histone deacetylase · inhibitors · lactams

[1] V. G. Allfrey, R. Faulkner, A. E. Mirsky, *Proc. Natl. Acad. Sci. USA* **1964**, *51*, 786–794.
[2] I. Gregoretti, Y.-M. Lee, H. V. Goodson, *J. Mol. Biol.* **2004**, *338*, 17–31.
[3] W. Fischle, V. Kiermer, F. Dequiedt, E. Verdin, *Biochem. Cell Biol.* **2001**, *79*, 337–348.
[4] W. K. Kelly, V. M. Richon, O. O'Connor, T. Curley, B. MacGregor-Curtelli, W. Tong, M. Klang, L. Schwartz, S. Richardson, E. Rosa, M. Drobnjak, C. Cordon-Cordo, J. H. Chiao, R. Rifkind, P. A. Marks, H. Scher, *Clin. Cancer Res.* **2003**, *9*, 3578–3588.
[5] a) K. N. Bhalla, *J. Clin. Oncol.* **2005**, *23*, 3971–3993; b) S. Minucci, P. G. Pelicci, *Nat. Rev. Cancer* **2006**, *6*, 38; c) C. Hildmann, D. Wegener, D. Riester, R. Hempel, A. Schober, J. Merana, L. Giurato, S. Guccione, T. K. Nielsen, R. Ficner, A. Schwienhorst, *J. Biotechnol.* **2006**, *124*, 258–270; d) A. V. Bieliauskas, M. K. H. Pflum, *Chem. Soc. Rev.* **2008**, *37*, 1402–1413.
[6] a) E. Hu, Z.-X. Chen, T. Fredrickson, Y. Zhu, R. Kirkpatrick, G.-F. Zhang, K. Johanson, C.-M. Sung, R.-G. Liu, J. Winkler, *J. Biol. Chem.* **2000**, *275*, 15254–15264; b) J. J. Buggy, M. L. Sideris, P. Mak, D. D. Lorimer, B. McIntosh, J. M. Clark, *Biochem. J.* **2000**, *350*, 199–205; c) M. Nakagawa, Y. Oda, T. Eguchi, S.-I. Aishima, T. Yao, F. Hosoi, Y. Basakv, M. Ono, M. Kuwano, M. Tanaka, M. Tsuneyoshi, *Oncol. Rep.* **2007**, *18*, 769–774.
[7] D. Waltregny, L. De Leval, W. Glénisson, S. Ly Tran, B. J. North, A. Bellahcène, U. Weidle, E. Verdin, V. Castronovo, *Am. J. Pathol.* **2004**, *165*, 553–564.
[8] I. Oehme, H. E. Deubzer, D. Wegener, D. Pickert, J. P. Linke, B. Hero, A. Kopp-Schneider, F. Westermann, S. M. Ulrich, A. von Deimling, M. Fischer, O. Witt, *Clin. Cancer Res.* **2009**, *15*, 91–99.
[9] D. Waltregny, W. Glénisson, S. Ly Tran, B. J. North, E. Verdin, A. Colige, V. Castronovo, *FASEB J.* **2005**, *19*, 966–968.
[10] K. L. Durst, B. Lutterbach, T. Kummalue, *Mol. Cell. Biol.* **2003**, *23*, 607–619.
[11] H. Lee, N. Sengupta, A. Villagra, N. Rezai-Zadeh, E. Seto, *Mol. Cell. Biol.* **2006**, *26*, 5259–5269.
[12] P. Gallinari, S. Di Marco, P. Jones, M. Pallaoro, C. Steinkühler, *Cell Res.* **2007**, *17*, 195–211.
[13] S. Balasubramanian, J. Ramos, W. Luo, M. Sirisiawad, E. Verner, J. J. Buggy, *Leukemia* **2008**, *22*, 1026–1034.
[14] W. K. Rasheed, R. W. Johonstone, H. M. Prince, *Expert Opin. Invest. Drugs* **2007**, *16*, 659–677.
[15] a) J. R. Somoza, R. J. Skene, B. A. Katz, C. Mol, J. D. Ho, A. J. Jennings, C. Luong, A. Arvai, J. J. Buggy, E. Chi, J. Tang, B. C. Sang, E. Verner, R. Wynands, E. M. Leahy, D. R. Dougan, G. Snell, M. Navre, M. W. Knuth, R. V. Swanson, D. E. McRee, L. W. Tari, *Structure* **2004**, *12*, 1325–1334; b) K. KrennHrubec, B. L. Marshall, M. Hedglin, E. Verdin, S. M. Ulrich, *Bioorg. Med. Chem. Lett.* **2007**, *17*, 2874–2878.
[16] E. Hu, E. Dul, C. M. Sung, Z. Chen, R. Kirkpatrick, G. F. Zhang, K. Johanson, R. Liu, A. Lago, G. Hofmann, R. Macarron, M. de Los Frailes, P. Perez, J. Krawiec, J. Winkler, M. Jaye, *J. Pharmacol. Exp. Ther.* **2003**, *307*, 720–728.
[17] G. Veinberg, M. Vorona, I. Shestakova, I. Kanepe, E. Lukevics, *Curr. Med. Chem.* **2003**, *10*, 1741–1757.
[18] M. I. Konaklieva, *Curr. Med. Chem.: Anti-Infect. Agents* **2002**, *1*, 215–238.
[19] F. Broccolo, G. Cainelli, G. Caltabiano, C. E. A. Cocuzza, C. G. Fortuna, P. Galletti, D. Giacomini, G. Musumarra, R. Musumeci, A. Quintavalla, *J. Med. Chem.* **2006**, *49*, 2804–2811.
[20] a) G. Cainelli, P. Galletti, S. Garbisa, D. Giacomini, L. Sartor, A. Quintavalla, *Bioorg. Med. Chem.* **2005**, *13*, 6120–6132; b) I. Dell'Aica, L. Sartor, P. Galletti, D. Giacomini, A. Quintavalla, F. Calabrese, C. Giacometti, E. Brunetta, F. Piazza, C. Agostini, S. Garbisa, *J. Pharmacol. Exp. Ther.* **2006**, *316*, 539–546.
[21] G. Cainelli, C. Angeloni, R. Cervellati, P. Galletti, D. Giacomini, S. Hrelia, R. Sinisi, *Chem. Biodiversity* **2008**, *5*, 811–829.
[22] M. Pavanetto, A. Zarpellon, D. Giacomini, P. Galletti, A. Quintavalla, G. Cainelli, A. Folda, G. Scutari, R. Deana, *Platelets* **2007**, *18*, 357–364.
[23] B. K. Banik, F. F. Becker, I. Banik, *Bioorg. Med. Chem.* **2004**, *12*, 2523–2528.
[24] D. Chen, S. C. Falsetti, M. Frezza, V. Milacic, A. Kazi, Q. C. Cui, T. E. Long, E. Turos, Q. P. Dou, *Cancer Lett.* **2008**, *268*, 63–69.
[25] S. Oh, J-C. Jung, M. A. Avery, *Z. Naturforsch., B: J. Chem. Sci.* **2007**, *62b*, 1459–1464.
[26] a) S. Dallavalle, R. Cincinelli, R. Nannei, L. Merlini, G. Morini, S. Penco, C. Pisano, L. Vesci, M. Barbarino, V. Zuco, M. De Cesare, F. Zunino, *Eur. J. Med. Chem.* **2009**, *44*, 1900–1912; b) R. Cincinelli, S. Dallavalle, R. Nannei, S. Carella, D. De Zani, L. Merlini, S. Penco, E. Garattini, G. Giannini, C. Pisano, L. Vesci, P. Carminati, V. Zuco, C. Zanchi, F. Zunino, *J. Med. Chem.* **2005**, *48*, 4931–4946.
[27] a) Screening was performed by Reaction Biology Corp. www.reactionbiology.com/; b) G. Giannini, T. Brunetti, R. Pezzi, G. Battistuzzi, M. Di Marzo, M. Marzi, W. Cabri, L. Vesci, C. Pisano, *Bioorg. Med. Chem. Lett.* **2009**, *19*, 2346–2349; c) G. Giannini, M. Marzi, M. DiMarzo, G. Battistuzzi, R. Pezzi, T. Brunetti, W. Cabri, L. Vesci, C. Pisano, *Bioorg. Med. Chem. Lett.* **2009**, *19*, 2840–2843.
[28] a) A. Vannini, C. Volpari, P. Gallinari, P. Jones, M. Mattu, A. Carfí, R. De Francesco, C. Steinkühler, S. Di Marco, *EMBO Rep.* **2007**, *8*, 879–884; b) A. Vannini, C. Volpari, G. Filocamo, E. Caroli Casavola, M. Brunetti, D. Renzoni, P. Chakravarty, C. Paolini, R. De Francesco, P. Gallinari, C. Steinkuhler, S. Di Marco, *Proc. Natl. Acad. Sci. USA* **2004**, *101*, 15064–15069.

[29] The azetidin-2-one was already reported as ligand in zinc complexes, see: F. Meyer, H. Pritzkow, *Eur. J. Inorg. Chem.* **2005**, 2346–2351.
[30] Y. Kozawa, M. Mori, *J. Org. Chem.* **2003**, *68*, 3064–3067.
[31] T. Aida, R. Legault, D. Dugat, T. Durst, *Tetrahedron Lett.* **1979**, *20*, 4993–4994.
[32] J. Eriksson, O. Åberg, B. Långström, *Eur. J. Org. Chem.* **2007**, 455–461.
[33] A. J. McNeil, G. E. S. Toombes, S. M. Gruner, E. Lobkovsky, D. B. Collum, S. V. Chandramouli, B. J. Vanasse, T. A. Ayers, *J. Am. Chem. Soc.* **2004**, *126*, 16559–16568.
[34] A. Urbach, G. G. Muccioli, E. Stern, D. M. Lambert, J. Marchand-Brynaert, *Bioorg. Med. Chem. Lett.* **2008**, *18*, 4163–4167.
[35] E. Hernandez, H. Hoberg, *J. Organomet. Chem.* **1987**, *327*, 429–436.
[36] J. L. Herrmann, R. H. Schlessinger, *Tetrahedron Lett.* **1973**, *14*, 2429–2432.
[37] R. Varala, R. Enugala, S. R. Adapa, *J. Iran. Chem. Soc.* **2007**, *4*, 370–374.
[38] P. Wipf, J. P. Maciejewski, *Org. Lett.* **2008**, *10*, 4383–4386.

Received: July 27, 2009
Revised: September 3, 2009
Published online on October 9, 2009

